Structural Engineering and Mechanics, *Vol. 71, No. 1 (2019) 37-43*
DOI: https://doi.org/10.12989/sem.2019.71.1.037

Effect of pre-magneto-electro-mechanical loads and initial curvature on the free vibration characteristics of size-dependent beam

M. Arefi*

Department of Solid Mechanic, Faculty of Mechanical Engineering, University of Kashan, Kashan 87317-51167, Iran

(Received November 8, 2018, Revised December 20, 2018, Accepted January 24, 2019)

Abstract. This paper studies application of modified couple stress theory and first order shear deformation theory to magneto-electro-mechanical vibration analysis of three-layered size-dependent curved beam. The curved beam is resting on Pasternak's foundation and is subjected to mechanical, magnetic and electrical loads. Size dependency is accounted by employing a small scale parameter based on modified couple stress theory. The magneto-electro-mechanical preloads are accounted in governing equations to obtain natural frequencies in terms of initial magneto-electro-mechanical loads. The analytical approach is applied to investigate the effect of some important parameters such as opening angle, initial electric and magnetic potentials, small scale parameter, and some geometric dimensionless parameters and direct and shear parameters of elastic foundation on the magneto-electro-elastic vibration responses.

Keywords: vibration Responses; modified couple stress; initial electric and magnetic potentials; length scale parameter

1. Introduction

To measure deformations or stresses in structures and coupled systems and also to perform a defined work, the piezoelectric materials are used as sensor or actuator in electro-mechanical systems. These effects are used frequently in electro-magneto-mechanical systems. These materials can be used in small scales such as micro or nano for some specific operations. To capture the various mechanical, vibrational, thermal and buckling analysis of piezoelectric and piezomagnetic structures in small scales, some non classical theories such as nonlocal Eringen elasticity theory, modified couple stress theory and strain gradient theory have been developed by various researchers. This paper aims to consider the effect of couple stress theory on the magneto-electro-mechanical vibration analysis of laminated curved beam integrated with piezomagnetic layers as sensor and actuator subjected to initially electric and magetic potentials. The literature review is presented to show that the subject of this paper needs some more consideration.

Radial vibration analysis of a curved beam was studied by Petyt and Fleischer (1971) using finite element method to present natural frequencies of curved beam for various boundary conditions such as simply supported, hinged and clamped ends. Surana *et al.* (1989) provided three dimensional nonlinear analysis of a curved beam using the total Lagrangian approach. Raveendranath *et al.* (2000) summarized some advantages and characteristics of a two-noded shear flexible curved beam element including three degree of freedom at each node based on curvilinear deep shell theory. The displacement field was assumed using a cubic polynomial function for radial and tangential displacements and section rotation. The results indicated that performance of the element is much superior to other elements of the same class. Effect of sinusoidal excitation was studied on the nonlinear buckling responses of clamped-clamped curved beam by Poon *et al.* (2002). Runge-Kutta numerical integration method was used for solution of the governing equations of motion. Shi (2005) analyzed bending behaviors of a piezoelectric and functionally graded curved actuator based on theory of piezo-elasticity subjected to an external voltage. The influence of power index of functionally graded material has been investigated on the results and the obtained results have been approved by comparison with finite element approach.

Piovan *et al.* (2015) presented dynamic analysis of magneto-electro-elastic curved beams. The aim of this work was to control motions and/or attenuate vibrations, for energy harvesting. The responses of curved beam were evaluated based on finite element method. One-dimensional beam theory of piezo-elasticity was employed by Kuang *et al.* (2007) in order to study static responses of a circular curved beam integrated with piezoelectric actuators. The obtained results have been verified by comparison with finite element results. Shi and Zhang (2008) studied bending analysis of a functionally graded piezoelectric curved beam subjected to external electric potential using theory of piezo-elasticity. The effect of variable curvature on the transient analysis of a curved piezoelectric beam with a piezoelectric vibration energy harvester was studied by Zhou *et al.* (2017). Arefi (2015) studied elastic solution of a curved beam made of functionally graded materials with various cross sections such as circular, rectangular and triangular. The influence of some important parameters such

*Corresponding author, Assistant Professor, Ph.D.
E-mail: arefi@kashanu.ac.ir

ISSN: 1225-4568 (Print), 1598-6217 (Online)

as non-homogeneous index and various cross sections has been investigated on the stress distribution of curved beam. Zhou *et al.* (2010) studied the piezoelectric laminated curved nano beams with variable curvature as an element of electromechanical systems. They modeled the curved beam using radial and tangential displacements and rotation. The influence of some geometrical parameters and patterns of layers was studied in detail. The influence of applied electric and magnetic potentials on the sandwich rod, beam and plates has been studied by researchers (Arefi and Zenkour (2017a-f), Arefi 2016, Arefi *et al.* 2018).

Vu-Bac *et al.* (2016) provided a sensitivity analysis for quantifying the influence of uncertain input parameters on uncertain model outputs. The effectiveness of this study were highlighted using numerical studies based on analytical functions. Hamida *et al.* (2018) provided a sensitivity analysis for identification of key input parameters affecting energy conversion factor of flexoelectric materials. The numerical results indicated that the flexoelectric constants are the most dominant factors influencing the uncertainties in the energy conversion factor. Ghasemi *et al.* (2018) presented a computational methodology for topology optimization of multi-material-based flexoelectric composites. They provided some numerical examples for two, three and four phase flexoelectric composites to demonstrate the flexibility of the model that can be obtained using multi-material topology optimization for flexoelectric composites. Some related works to optimization and computational methods of flexoelectric and piezoelectric structures were studied by various researchers (Ghasemi *et al.* 2017; Thai *et al*. 2017; Nanthakumar *et al*. 2016; Nguyen *et al*. 2018)

A comprehensive literature review on the important works related to some significant topics such as electro-magneto-elastic problems, size dependent analyses, magneto-electro-elastic vibration and some related works on them in micro and nano scales and curved structures has been completed above. One can conclude that although some works on the curved beam have been reported by various researchers, however it is investigated that there is no comprehensive work on application of first order shear deformation theory and modified couple stress theory to the magneto-electro-elastic vibration analysis of laminated micro curved beam subjected to electro-magneto-mechanical loads. The governing equations of motion are derived based on Hamilton's principle. The significant numerical results including free vibration characteristics are presented in terms of important parameters such as opening angle, micro length scale parameter, initial electric and magnetic potentials and two parameters of Pasternak's foundation and.

2. Formulation

To capture the influence of micro scales on the vibration responses of curved structure (Figure 1), modified couple stress theory is employed. Based on this theory, strain energy is expressed as follows:

$$U_s = \frac{1}{2}\int_v \left(\sigma_{ij}\varepsilon_{ij} + m_{ij}\chi_{ij} - D_i E_i - B_i H_i\right) dV \tag{1}$$

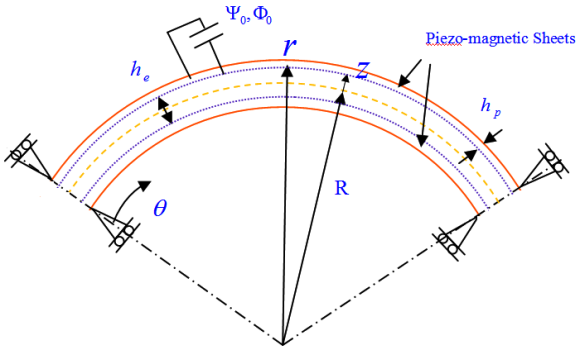

Fig. 1 The schematic figure of a three-layer curved nanobeam

In which σ_{ij} and ε_{ij} are the components of the stress and strain tensors, m_{ij} are the components of the deviatoric part of the symmetric couple stress tensor and χ_{ij} are the components of the symmetric curvature tensor that are defined as follows:

$$m_{ij} = \frac{E}{1+\nu} l^2 \chi_{ij} \quad \chi = \frac{1}{2}\left(\nabla\vec{\theta} + \left(\nabla\vec{\theta}\right)^T\right) \tag{2}$$

In which l is the material length scale parameter and θ_i are the components of the rotation vector. In Eq. 1, D_i, B_i are electric displacement and magnetic induction components and E_i, H_i are electric and magnetic field components.

The electric displacement and magnetic induction components along the radial and circumferential directions are derived as:

$$\begin{aligned} {D_r}^p &= {e_{r\theta\theta}}^p \varepsilon_\theta + {\epsilon_{rr}}^p E_r + {m_{rr}}^p H_r \\ {D_\theta}^p &= {e_{\theta r\theta}}^p \gamma_{r\theta} + {\epsilon_{\theta\theta}}^p E_\theta + {m_{\theta\theta}}^p H_\theta \\ {B_r}^p &= {q_{r\theta\theta}}^p \varepsilon_\theta + {m_{rr}}^p E_r + {\mu_{rr}}^p H_r \\ {B_\theta}^p &= {q_{\theta r\theta}}^p \gamma_{r\theta} + {m_{\theta\theta}}^p E_\theta + {\mu_{\theta\theta}}^p H_\theta \end{aligned} \tag{3}$$

in which m_{ij} and μ_{ij} are dielectric and electromagnetic coefficients. In order to complete constitutive mechanical, electrical and magnetic loads, the electric and magnetic potentials should be completed. For this aim, the electric and magnetic potentials are defined as (Arefi and Zenkour 2017a-f, Arefi 2016, Arefi *et al.* 2018)

$$\begin{aligned} \breve{\psi}(r,\theta) &= \frac{2\psi_0}{h_p}\rho - \psi(\theta)\cos\left(\frac{\pi}{h_p}\rho\right) \\ \breve{\phi}(r,\theta) &= \frac{2\phi_0}{h_p}\rho - \phi(\theta)\cos\left(\frac{\pi}{h_p}\rho\right) \end{aligned} \tag{4}$$

In which, ψ_0, ϕ_0 are applied electric and magnetic potentials, $\rho = \zeta \pm \frac{h_e}{2} \pm \frac{h_p}{2}$ for top and bottom piezo-magnetic face-sheets, respectively. The first term in electric and magnetic potentials is applied electric and magnetic potentials and second terms are used for description of homogeneous electrical and magnetic boundary conditions.

Electric and magnetic fields are derived based on following relation in terms of electric and magnetic potentials (Arefi and Zenkour (2017a-f), Arefi 2016, Arefi *et al.* 2018).

$$\begin{aligned} \mathrm{E_r} &= -\frac{\partial\breve{\psi}}{\partial \mathrm{r}}, \mathrm{E_\theta} = -\frac{1}{\mathrm{r}}\frac{\partial\breve{\psi}}{\partial\theta} \\ \mathrm{H_r} &= -\frac{\partial\breve{\phi}}{\partial \mathrm{r}}, \mathrm{H_\theta} = -\frac{1}{\mathrm{r}}\frac{\partial\breve{\phi}}{\partial\theta} \end{aligned} \tag{5}$$

In this stage and using the Hamilton's principle $\int \delta(T - U + V)dt = 0$, we can derive the governing equations of motion. The variation of strain energy δU is defined as:

$$\delta U = \iiint_v \left(\sigma_{ij}\delta\varepsilon_{ij} - D_i\delta E_i - B_i\delta H_i + m_{ij}\chi_{ij}\right)\mathrm{d}V. \tag{6}$$

The work performed by external works including mechanical, electrical and magnetic loads is expressed as follows:

$$W_{Ext} = \int_\theta (N_0 + N_E + N_M)\left(\frac{1}{r}\frac{du_\theta}{d\theta}\right)^2 \mathrm{r}\mathrm{d}\theta. \tag{7}$$

In which $N_0.N_E.N_M$ are mechanical, electrical and magnetic pre-loads. N_0 is direct pre-mechanical loads and remained terms are pre-electrical and mechanical loads that are defined as:

$$\begin{aligned} \{N_E, N_M\} = &\int_{-\frac{h_e}{2}-h_p}^{-\frac{h_e}{2}} \{\frac{2\psi_0}{h_p}e_{\theta\theta\theta}{}^p, \frac{2\phi_0}{h_p}q_{\theta\theta\theta}{}^p\}\mathrm{d}z \\ &+ \int_{\frac{h_e}{2}}^{\frac{h_e}{2}+h_p} \{\frac{2\psi_0}{h_p}e_{\theta\theta\theta}{}^p, \frac{2\phi_0}{h_p}q_{\theta\theta\theta}{}^p\}\mathrm{d}z. \end{aligned} \tag{8}$$

The terms defined in Eq. 8 show pre-loads due to electrical and mechanical loads. Substitution of strain energy, kinetic energy and external woks into Hamilton's principle leads to final governing equations of motion as follow:

$$\begin{aligned} &\delta u_r: -N_{\theta\theta} + \frac{dN_{r\theta}}{d\theta} + \frac{1}{4}\frac{dM_{rz}{}^\chi}{d\theta} + \frac{1}{4}\frac{d^2M_{\theta z}{}^\chi}{d\theta^2} \\ &+\left(K_1u_r - K_2\frac{1}{\left(R - \frac{h_e}{2} - h_p\right)^2}\frac{d^2u_r}{d\theta^2}\right)\left(R - \frac{h_e}{2} - h_p\right) \\ &-(N_0 + N_E + N_M)\left(\frac{1}{r^2}\frac{d^2u_r}{d\theta^2}\right)\left(R + \frac{h_e}{2} + h_p\right) = A_1\ddot{u}_r \\ &\delta u_\theta: \frac{dN_{\theta\theta}}{d\theta} + N_{r\theta} + \frac{1}{4}\frac{dM_{\theta z}{}^\chi}{d\theta} - \frac{1}{4}M_{rz}{}^\chi = A_1\ddot{u}_\theta + A_2\ddot{\vartheta} \\ &\delta\chi: \frac{dM_{\theta\theta}}{d\theta} - (RN_{r\theta} + M_{r\theta}) + M_{r\theta} - \frac{1}{2}N_{\theta\theta}{}^\chi + \frac{1}{4}\frac{dN_{r\theta}{}^\chi}{d\theta} \\ &+\frac{1}{4}M_{rz}{}^\chi R + \frac{1}{4}\frac{dN_{\theta z}{}^\chi}{d\theta} + \frac{1}{4}\frac{dP_{\theta z}{}^\chi}{d\theta} = A_2\ddot{u}_\theta + A_3\ddot{\vartheta} \\ &\delta\psi: -\bar{D}_r - \frac{d\bar{D}_\theta}{d\theta} = 0 \\ &\delta\phi: -\bar{B}_r - \frac{d\bar{B}_\theta}{d\theta} = 0 \end{aligned} \tag{9}$$

Substitution of resultant components in terms of basic relations into governing relations leads to:

$$\begin{aligned} &\delta u_r: -\frac{1}{4}A_{33}\frac{d^4u_r}{d\theta^4} + \left[\frac{1}{4}A_{35} + A_{11}\right]\frac{d^2u_r}{d\theta^2} - A_4u_r \\ &+\frac{1}{4}A_{33}\frac{d^3u_\theta}{d\theta^3} \\ &+\left[\frac{1}{4}A_{35} - A_4 - A_{11}\right]\frac{du_\theta}{d\theta} + \frac{1}{4}[A_{32} + A_{34}]\frac{d^3\vartheta}{d\theta^3} \\ &+\left[A_{12} - A_{13} - A_5 - \frac{1}{4}A_{35}R\right]\frac{d\vartheta}{d\theta} - A_{14}\frac{d^2\psi}{d\theta^2} - A_6\psi \\ &-A_{15}\frac{d^2\phi}{d\theta^2} \\ &-A_7\phi + \left(K_1u_r - K_2\frac{1}{\left(R - \frac{h_e}{2} - h_p\right)^2}\frac{d^2u_r}{d\theta^2}\right)\left(R - \frac{h_e}{2}\right. \\ &\left.- h_p\right) \\ &-(N_0 + N_E + N_M)\left(\frac{1}{r^2}\frac{d^2u_r}{d\theta^2}\right)\left(R + \frac{h_e}{2} + h_p\right) = A_1\ddot{u}_r \\ &\delta u_\theta: -\frac{1}{4}A_{33}\frac{d^3u_r}{d\theta^3} + \left[A_4 + A_{11} - \frac{1}{4}A_{35}\right]\frac{du_r}{d\theta} \\ &+\left[A_4 + \frac{1}{4}A_{33}\right]\frac{d^2u_\theta}{d\theta^2} - \left[A_{11} + \frac{1}{4}A_{35}\right]u_\theta \\ &+\left[A_5 + \frac{1}{4}A_{32} + \frac{1}{4}A_{34}\right]\frac{d^2\vartheta}{d\theta^2} + \left[A_{12} - A_{13} + \frac{1}{4}A_{35}R\right]\vartheta \\ &+[A_6 - A_{14}]\frac{d\psi}{d\theta} + [A_7 - A_{15}]\frac{d\phi}{d\theta} = A_1\ddot{u}_\theta + A_2\ddot{\chi} \\ &\delta\vartheta: -\frac{1}{4}[A_{36} + A_{33}]\frac{d^3u_r}{d\theta^3} + \left[\frac{1}{4}RA_{35} + A_5\right]\frac{du_r}{d\theta} \\ &-RA_{11}\frac{du_r}{d\theta} \\ &+\left[A_5 + \frac{1}{4}A_{33} + \frac{1}{4}A_{36}\right]\frac{d^2u_\theta}{d\theta^2} + [RA_{11} + \frac{1}{4}RA_{35}]u_\theta \\ &+\left[A_8 + \frac{1}{2}A_{32} + \frac{1}{2}A_{34} + \frac{1}{4}A_{37}\right]\frac{d^2\vartheta}{d\theta^2} \\ &+\left[-RA_{12} + RA_{13} - A_{32} - \frac{1}{4}R^2A_{35}\right]\vartheta + A_9\frac{d\psi}{d\theta} \\ &+RA_{14}\frac{d\psi}{d\theta} + A_{10}\frac{d\phi}{d\theta} + RA_{15}\frac{d\phi}{d\theta} = A_2\ddot{u}_\theta + A_3\ddot{\chi} \\ &\delta\psi: -A_{23}\frac{d^2u_r}{d\theta^2} - A_{16}u_r + [A_{23} - A_{16}]\frac{du_\theta}{d\theta} \\ &+[A_{25} - A_{17} - A_{24}]\frac{d\chi}{d\theta} - A_{29}\frac{d^2\psi}{d\theta^2} \\ &+A_{18}\psi \\ &-A_{30}\frac{d^2\phi}{d\theta^2} + A_{19}\phi = -D_\psi - D_\phi \\ &\delta\phi: -A_{26}\frac{d^2u_r}{d\theta^2} - A_{20}u_r + [A_{26} - A_{20}]\frac{du_\theta}{d\theta} + [A_{28} \\ &-A_{21} - A_{27}]\frac{d\chi}{d\theta} - A_{30}\frac{d^2\psi}{d\theta^2} + A_{19}\psi \\ &-A_{31}\frac{d^2\phi}{d\theta^2} + A_{22}\phi = -B_\psi - B_\phi \end{aligned} \tag{10}$$

Table 1 Variation of first, second and third natural frequencies (in GHz) in terms of applied voltage

Ψ_0	ω_1(1st mode)	ω_2(2nd mode)	ω_3(3rd mode)
0	423.30	1066.87	1724.66
10	423.38	1067.01	1724.86
20	423.46	1067.15	1725.06

Table 2 Variation of first, second and third natural frequencies (in GHz) in terms of applied magnetic

Φ_0	ω_1(1st mode)	ω_2(2nd mode)	ω_3(3rd mode)
0	423.30	1066.87	1724.66
0.1	423.20	1066.69	1724.41
0.2	423.09	1066.51	1724.16

3. Solution procedure

In this section, the solution procedure for electro-magneto-mechanical vibration results is developed. The proposed solutions for a simply-supported curved sandwich beam are expressed as:

$$\begin{Bmatrix} (u_\theta, \vartheta) \\ (u_r.\psi, \phi) \end{Bmatrix} = \sum_{m=1.3.5} e^{i\omega t} \begin{Bmatrix} (U_\theta, \vartheta)\cos(\alpha\theta) \\ (U_r, \Psi, \Phi)\sin(\alpha\theta) \end{Bmatrix} \quad (11)$$

in which $\alpha = {m\pi R}/{L}$ and ω is natural frequency of the problem. This solution is applicable for simply-supported boundary conditions and homogeneous electric and magnetic boundary conditions. For other boundary conditions, the numerical and semi-analytical methods should be developed. Substitution of proposed solution into governing equations of motion leads to below equation:

$$[K]\{X\} = \omega^2[M]\{X\} \quad (12)$$

In which $\{X\} = \{U_r, U_\theta, \mathrm{X}, \Psi, \Phi\}$ is an unknown vector corresponding to five unknown functions, $[K]$ is stiffness matrix and $[M]$ is mass matrix. Solution of characteristic equation $Det\{[K] - \omega^2[M]\} = 0$ leads to natural frequencies of the problem.

4. Results and discussions

In this section, the numerical results of the problem are presented. The electro-magneto-elastic vibration results are presented in this section in terms of important parameters of the sandwich curved beam such as length scale parameter, applied electric and magnetic potentials, direct and shear parameters of Pasternak's foundation and opening angle. To account length scale parameter, a dimensionless parameter l is defined as: $\mathrm{l}' = \mathrm{l} \times 17.65\mu\mathrm{m}$.

Tables 1 and 2 list variation of first, second and third natural frequencies in terms of various values of applied electric and magnetic potentials, respectively. It is observed that the natural frequencies are increased with increase of applied electric potential and decrease of magnetic potential. One can see that these behaviors are in accordance with results of literature (Liu *et al.* 2013).

Table 3 Variation of first, second and third natural frequencies (in GHz) in terms of small scale parameter

l	ω_1(1st mode)	ω_2(2nd mode)	ω_3(3rd mode)
0.9	394.26	1022.55	1675.52
0.95	409.05	1045.29	1700.61
1	423.30	1066.87	1724.67

Table 4 Variation of first, second and third natural frequencies (in GHz) in terms of applied magnetic

$\theta = {L}/{R}$	ω_1(1st mode)	ω_2(2nd mode)	ω_3(3rd mode)
0/8	578.07	1396.71	2211.95
1	423.30	1066.87	1724.66
1/2	325.28	847.39	1396.71

Table 5 Variation of first, second and third natural frequencies (in GHz) in terms of applied magnetic

N_0	ω_1(1st mode)	ω_2(2nd mode)	ω_3(3rd mode)
0	423.30	1066.87	1724.66
1E3	422.39	1065.30	1722.42
1E4	414.127	1051.04	1702.15

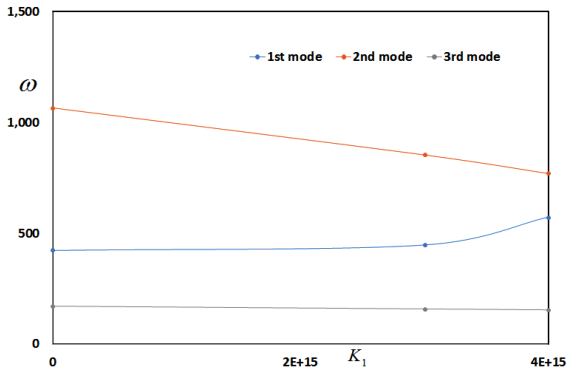

Fig. 2 Variation of first, second and third natural frequencies (in GHz) in terms of direct parameter of foundationK_1

Table 3 lists the influence of small scale parameter on the free vibration responses of sandwich curved beam. One can conclude that with increase of small scale parameter *l*, the stiffness of structure is increased and consequently the natural frequency is increased. It is concluded that this conclusion is completely in accordance with results of literature (Arefi *et al.* 2018).

Variation of first three natural frequencies of sandwich curved beam in terms of various opening angles is listed in Table 4. One can conclude that with increase of opening angle, the natural frequencies are decreased significantly.

Table 5 lists variation of first three natural frequencies of sandwich curved beam in terms of various mechanical pre-loads (N_0). One can conclude that increase of pre-loads leads to decrease of fundamental natural frequency.

Figures 2 and 3 show variation of first three natural frequencies of sandwich curved beam in terms of direct and shear parameters of Pasternak's foundation, respectively. It

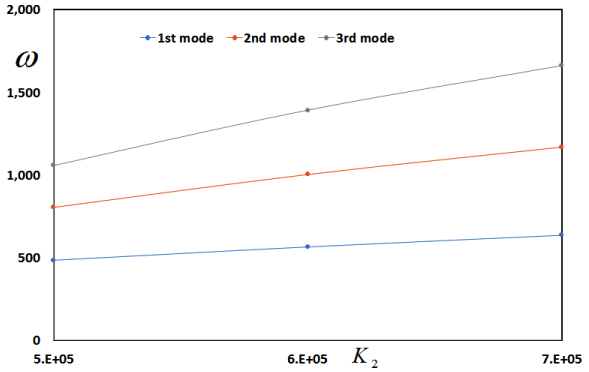

Fig. 3 Variation of first, second and third natural frequencies (in GHz) in terms of shear parameter of foundationK_2.

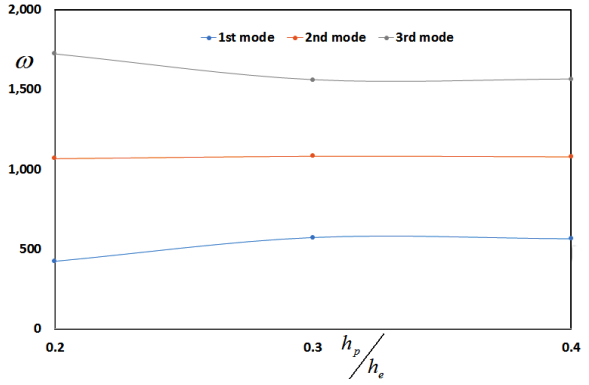

Fig. 4 Variation of first, second and third natural frequencies (in GHz) in terms of direct parameter of foundationh_p/h_e

is observed that with increase of two parameters, the fundamental natural frequencies are increased significantly. It is concluded that with increase of both parameters of foundation, the stiffness is increased and consequently the fundamental natural frequencies are increased significantly.

Figure 4 shows variation of first three natural frequencies of sandwich curved beam in terms of piezoelectric to core thickness ratio h_p/h_e. The numerical results indicate that with increase of h_p/h_e, the fundamental natural frequencies are increased significantly. It is concluded that with increase of piezoelectric to core thickness ratio h_p/h_e, the portion of core in bending stiffness of sandwich structure is increased and consequently the natural frequencies are increased.

5. Conclusion

Magneto-electro-elastic vibration analysis of a three-layered curved beam was studied in this paper based on modified couple stress formulation and first-order shear deformation theory. Hamilton's Principle was used to derive governing equations of motion in terms of displacement field and magnetic and electric fields. The numerical results were presented in terms of length scale parameter, opening angle, initial electric and magnetic potentials, direct and shear parameters of foundation and piezoelectric thickness to core thickness ratio. Some significant outputs of this analysis are expressed as follows:

Initial electric and magnetic potentials lead to significant changes of natural frequencies. It is observed that the natural frequencies are increased with increase of initial electric potential and decrease of magnetic potential.

The numerical results show that with increase of length scale parameter, the stiffness of curved beam is increased and consequently the natural frequencies are increased significantly.

Investigation on the effect of opening angle indicates that with increase of opening angle of curved beam, the stiffness is decreased and then the natural frequencies are decreased.

The influence of piezoelectric to core thickness ratio h_p/h_e was studied on natural frequencies for the case that total thickness of curved beam to be constant. It is concluded that with increase of piezoelectric to core thickness ratioh_p/h_e, the bending stiffness of sandwich structure is increased and consequently the natural frequencies are increased.

References

Arefi, M. (2015), "Elastic solution of a curved beam made of functionally graded materials with different cross sections", *Steel. Compos. Struct.*, **18**(3), 659-672. http://doi.org/10.12989/scs.2015.18.3.659.

Arefi, M. and Zenkour, A.M. (2017a), "Effect of thermo-magneto-electro-mechanical fields on the bending behaviors of a three-layered nanoplate based on sinusoidal shear-deformation plate theory", *J. Sandw. Struct. Mater.* https://doi.org/10.1177/1099636217697497.

Arefi, M. and Zenkour, A.M. (2017b), "Employing the coupled stress components and surface elasticity for nonlocal solution of wave propagation of a functionally graded piezoelectric Love nanorod model", *J. Intel. Mater. Syst. Struct.*, **28**(17), 2403-2413. https://doi.org/10.1177/1045389X17689930.

Arefi, M. and Zenkour, A.M. (2017c), "Influence of magneto-electric environments on size-dependent bending results of three-layer piezomagnetic curved nanobeam based on sinusoidal shear deformation theory", *J. Sandw. Struct. Mater.*, https://doi.org/10.1177/1099636217723186.

Arefi, M. and Zenkour, A.M. (2017d), "Transient analysis of a three-layer microbeam subjected to electric potential", *Int. J. Smart. Nano. Mater.*, **8**(1), 20-40. https://doi.org/10.1080/19475411.2017.1292967.

Arefi, M. and Zenkour, A.M. (2017e), "Transient sinusoidal shear deformation formulation of a size-dependent three-layer piezo-magnetic curved nanobeam", *Acta. Mech.*, **228**(10), 3657-3674. https://doi.org/10.1007/s00707-017-1892-6.

Arefi, M. and Zenkour, A.M. (2017f), "Size-dependent free vibration and dynamic analyses of piezo-electro-magnetic sandwich nanoplates resting on viscoelastic foundation", *Phys. B. Cond. Matt.*, **521**, 188-197. https://doi.org/10.1016/j.physb.2017.06.066.

Arefi, M. (2016), "Analysis of wave in a functionally graded magneto-electro-elastic nano-rod using nonlocal elasticity model subjected to electric and magnetic potentials", *Acta Mech.*, **227**, 2529-2542. https://doi.org/10.1007/s00707-016-1584-7.

Arefi, M., Zamani, M.H. and Kiani, M., (2018), "Size-dependent free vibration analysis of three-layered exponentially graded nanoplate with piezomagnetic face-sheets resting on Pasternak's

foundation", *J. Intel. Mater. Syst. Struct.,* **29**(5), 774-786. https://doi.org/10.1177/1045389X17721039.

Ghasemi, H. Park, H.S. and Rabczuk, T. (2017), "A level-set based IGA formulation for topology optimization of flexoelectric materials", *Comput. Meth. Appl. Mech. Eng.*, **313**, 239-258. https://doi.org/10.1016/j.cma.2016.09.029.

Ghasemi, H. Park, H.S. and Rabczuk, T. (2018), "A multi-material level set-based topology optimization of flexoelectric composites", *Comput. Meth. Appl. Mech. Eng.,* **332**, 47-62. https://doi.org/10.1016/j.cma.2017.12.005.

Hamdia, K.M. Silani, M. Zhuang, X. He, P. and Rabczuk, T. (2017), "Stochastic analysis of the fracture toughness of polymeric nanoparticle composites using polynomial chaos expansions", *Int. J. Fract.,* **206**(2) 215-227. https://doi.org/10.1007/s10704-017-0210-6.

Hamdia, K.M. Ghasemi, H. Zhuang, X. Alajlan, N. and Rabczuk, T. (2018), "Sensitivity and uncertainty analysis for flexoelectric nanostructures", *Comput. Meth. Appl. Mech. Eng.,* **337**, 95-109. https://doi.org/10.1016/j.cma.2018.03.016.

Kuang, Y.D., Li, G.Q., Chen, C.Y. and Min, Q. (2007), "The static responses and displacement control of circular curved beams with piezoelectric actuators", *Smart. Materi. Struct.,* **16**, 1016-1024.

Liu, C., Ke, L.L., Wang, Y.S., Yang, J. and Kitipornchai, S. (2013), "Thermo-electro-mechanical vibration of piezoelectric nanoplates based on the nonlocal theory", *Compos. Struct.,* **106**, 167-174. https://doi.org/10.1016/j.compstruct.2013.05.031.

Nanthakumar, S.S., Lahmer, T., Zhuang, X., Zi, G. and Rabczuk, T. (2016), "Detection of material interfaces using a regularized level set method in piezoelectric structures", *Inv. Prob. Sci. Eng.,* **24**(1), 153-176. https://doi.org/10.1080/17415977.2015.1017485.

Nguyen, B.H., Zhuang, X. and Rabczuk, T. (2018), "Numerical model for the characterization of Maxwell-Wagner relaxation in piezoelectric and flexoelectric composite material", *Comput. Struct.,* **208**, 75-91. https://doi.org/10.1016/j.compstruc.2018.05.006.

Petyt, M. and Fleischer, C.C. (1971), "Free vibration of a curved beam", *J. Sound. Vib.* **18**(1), 17-30. https://doi.org/10.1016/0022-460X(71)90627-4.

Piovan, M.T., Olmedo, J.F. and Sampaio, R. (2015), "Dynamics of magneto electro elastic curved beams: Quantification of parametric uncertainties", *Compos. Struct.,* **133**, 621-629. https://doi.org/10.1016/j.compstruct.2015.07.084.

Poon, W.Y., Ng, C.F. and Lee, Y.Y. (2002), "Dynamic stability of a curved beam under sinusoidal loading", *Proc. Inst. Mech. Eng. Part G: J. Aer. Eng.,* **216**(4), 209-217. https://doi.org/10.1243/09544100260369740.

Raveendranath, P., Singh, G. and Pradhan, B. (2000), "Free vibration of arches using a curved beam element based on a coupled polynomial displacement field", *Comput. Struct.,* **78**(4), 583-590. https://doi.org/10.1016/S0045-7949(00)00038-9.

Raveendranath, P., Singh, G. and Pradhan, B. (1999), "A two-noded locking–free shear flexible curved beam element", *Int. J. Num. Meth. Eng.*, **44**(2), 265-280. https://doi.org/10.1002/(SICI)1097-0207(19990120)44:2<265::AID-NME505>3.0.CO;2-K

Shi, Z.F. (2005), "Bending behavior of piezoelectric curved actuator", *Smart. Materi. Struct*. **14**, 835-842.

Shi, Z.F. and Zhang, T. (2008), "Bending analysis of a piezoelectric curved actuator with a generally graded property for the piezoelectric parameter", *Smart. Materi. Struct.,* **17**, 045018.

Surana, K.S. and Sorem, R.M. (1989), "Geometrically non-linear formulation for three dimensional curved beam elements with large rotations", *Int. J. Num. Meth. Eng.,* **28**(1), 43-73. https://doi.org/10.1002/nme.1620280106.

Thai, T.Q., Rabczuk, T. and Zhuang, X. (2017), "A large deformation isogeometric approach for flexoelectricity and soft materials", *Comput. Meth. Appl. Mech. Eng.,* **341**, 718-739. https://doi.org/10.1016/j.cma.2018.05.019.

Vu-Bac, N., Lahmer, T., Zhuang, X., Nguyen-Thoi, T. and Rabczuk, T. (2016), "A software framework for probabilistic sensitivity analysis for computationally expensive models", *Adv. Eng. Softw.,* **100**, 19-31. https://doi.org/10.1016/j.advengsoft.2016.06.005.

Zhou, Y., Nyberg, T.R., Xiong, G., Zhou, H. and Li, S. (2017), "Precise deflection analysis of laminated piezoelectric curved beam", *J. Intel. Mater. Syst. Struct,* **27**(16), 2179-2198. https://doi.org/10.1177/1045389X15624797.

Zhou, Y., Dong, Y. and Li, S. (2010) "Analysis of a Curved Beam MEMS Piezoelectric Vibration Energy Harvester", *Adv. Mater. Res.,* **139-141**, 1578-1581. https://doi.org/10.4028/www.scientific.net/AMR.139-141.1578.

CC

Appendix

$$\{A_4, A_5, A_8\} = \int_{-\frac{h_e}{2}}^{+\frac{h_e}{2}} \frac{C_{\theta\theta\theta\theta}}{(R+\zeta)}\{1, z, z^2\}\mathrm{d}z + \int_{-\frac{h_e}{2}-h_p}^{-\frac{h_e}{2}} \frac{C_{\theta\theta\theta\theta}{}^p}{(R+z)}\{1, z, z^2\}\mathrm{d}z + \int_{\frac{h_e}{2}}^{\frac{h_e}{2}+h_p} \frac{C_{\theta\theta\theta\theta}{}^p}{(R+z)}\{1, z, z^2\}\mathrm{d}z$$

$$\{A_6, A_7, A_9, A_{10}\} = \int_{-\frac{h_e}{2}-h_p}^{-\frac{h_e}{2}} \frac{\pi}{h_p}\sin\left(\frac{\pi}{h_p}\rho\right)\{e_{\theta\theta r}{}^p, q_{\theta\theta r}{}^p, z e_{\theta\theta r}{}^p, z q_{\theta\theta r}{}^p\}\mathrm{d}z + \int_{\frac{h_e}{2}}^{\frac{h_e}{2}+h_p} \frac{\pi}{h_p}\sin\left(\frac{\pi}{h_p}\rho\right)\{e_{\theta\theta r}{}^p, q_{\theta\theta r}{}^p, z e_{\theta\theta r}{}^p, z q_{\theta\theta r}{}^p\}\mathrm{d}z$$

$$\{A_{11}, A_{12}, A_{13}\} = \int_{-\frac{h_e}{2}}^{+\frac{h_e}{2}} \frac{C_{r\theta r\theta}}{(R+z)}\{1, (R+z), z\}\mathrm{d}z + \int_{-\frac{h_e}{2}-h_p}^{-\frac{h_e}{2}} \frac{C_{r\theta r\theta}{}^p}{(R+z)}\{1, (R+z), z\}\mathrm{d}z + \int_{\frac{h_e}{2}}^{\frac{h_e}{2}+h_p} \frac{C_{r\theta r\theta}{}^p}{(R+z)}\{1, (R+z), z\}\mathrm{d}z$$

$$\{A_{14}, A_{15}\} = \int_{-\frac{h_e}{2}-h_p}^{-\frac{h_e}{2}} \frac{\cos\left(\frac{\pi}{h_p}\rho\right)}{(R+z)}\{e_{r\theta\theta}{}^p, q_{r\theta\theta}{}^p\}\mathrm{d}z + \int_{\frac{h_e}{2}}^{\frac{h_e}{2}+h_p} \frac{\cos\left(\frac{\pi}{h_p}\rho\right)}{(R+z)}\{e_{r\theta\theta}{}^p, q_{r\theta\theta}{}^p\}\mathrm{d}z$$

$$\{N_\psi, N_\phi, M_\psi, M_\phi\} = \int_{-\frac{h_e}{2}-h_p}^{-\frac{h_e}{2}} \{\frac{2\psi_0}{h_p}e_{\theta\theta\theta}{}^p, \frac{2\phi_0}{h_p}q_{\theta\theta\theta}{}^p, \frac{2\psi_0}{h_p}z e_{\theta\theta\theta}{}^p, \frac{2\phi_0}{h_p}z q_{\theta\theta\theta}{}^p\}(+ \int_{\frac{h_e}{2}}^{\frac{h_e}{2}+h_p} \{\frac{2\psi_0}{h_p}e_{\theta\theta\theta}{}^p, \frac{2\phi_0}{h_p}q_{\theta\theta\theta}{}^p, \frac{2\psi_0}{h_p}z e_{\theta\theta\theta}{}^p, \frac{2\phi_0}{h_p}z q_{\theta\theta\theta}{}^p\}($$

$$\{A_{16}, A_{17}, A_{20}, A_{21}\} = \int_{-\frac{h_e}{2}-h_p}^{-\frac{h_e}{2}} \frac{\pi}{h_p}\sin\left(\frac{\pi}{h_p}\rho\right)\{e_{r\theta\theta}{}^p, z e_{r\theta\theta}{}^p, q_{r\theta\theta}{}^p, z q_{r\theta\theta}{}^p\}\mathrm{d}\zeta + \int_{\frac{h_e}{2}}^{\frac{h_e}{2}+h_p} \frac{\pi}{h_p}\sin\left(\frac{\pi}{h_p}\rho\right)\{e_{r\theta\theta}{}^p, z e_{r\theta\theta}{}^p, q_{r\theta\theta}{}^p, z q_{r\theta\theta}{}^p\}\mathrm{d}z$$

$$\{A_{18}, A_{19}, A_{22}\} = \int_{-\frac{h_e}{2}-h_p}^{-\frac{h_e}{2}} (R+z)\left[\frac{\pi}{h_p}\sin\left(\frac{\pi}{h_p}\rho\right)\right]^2\{\epsilon_{rr}{}^p, m_{rr}{}^p, \mu_{rr}{}^p\}\mathrm{d}z + \int_{\frac{h_e}{2}}^{\frac{h_e}{2}+h_p} (R+z)[\frac{\pi}{h_p}\sin\left(\frac{\pi}{h_p}\rho\right)]^2\{\epsilon_{rr}{}^p, m_{rr}{}^p, \mu_{rr}{}^p\}\mathrm{d}z$$

$$\{D_\psi, D_\phi, B_\psi, B_\phi\} = \int_{-\frac{h_e}{2}-h_p}^{-\frac{h_e}{2}} (R + z)\{\frac{2\psi_0}{h_p}\epsilon_{rr}{}^p, \frac{2\phi_0}{h_p}m_{rr}{}^p, \frac{2\psi_0}{h_p}m_{rr}{}^p, \frac{2\phi_0}{h_p}\mu_{rr}{}^p\}\mathrm{d}z + \int_{\frac{h_e}{2}}^{\frac{h_e}{2}+h_p} (R + z)\{\frac{2\psi_0}{h_p}\epsilon_{rr}{}^p, \frac{2\phi_0}{h_p}m_{rr}{}^p, \frac{2\psi_0}{h_p}m_{rr}{}^p, \frac{2\phi_0}{h_p}\mu_{rr}{}^p\}\mathrm{d}z$$

$$\{A_{23}, A_{24}, A_{25}, A_{26}, A_{27}, A_{28}\} = \int_{-\frac{h_e}{2}-h_p}^{-\frac{h_e}{2}} \frac{\cos\left(\frac{\pi}{h_p}\rho\right)}{(R+z)}\{e_{\theta r\theta}{}^p, (R+z)e_{\theta r\theta}{}^p, z e_{\theta r\theta}{}^p, q_{\theta r\theta}{}^p, (R + z)q_{\theta r\theta}{}^p, z q_{\theta r\theta}{}^p\}\mathrm{d}z + \int_{\frac{h_e}{2}}^{\frac{h_e}{2}+h_p} \frac{\cos\left(\frac{\pi}{h_p}\rho\right)}{(R+z)}\{e_{\theta r\theta}{}^p, (R + z)e_{\theta r\theta}{}^p, z e_{\theta r\theta}{}^p, q_{\theta r\theta}{}^p, (R + z)q_{\theta r\theta}{}^p, z q_{\theta r\theta}{}^p\}\mathrm{d}z$$

$$\{A_{29}, A_{30}, A_{31}\} = \int_{-\frac{h_e}{2}-h_p}^{-\frac{h_e}{2}} \frac{[\cos\left(\frac{\pi}{h_p}\rho\right)]^2}{(R+z)}\{\epsilon_{\theta\theta}{}^p, m_{\theta\theta}{}^p, \mu_{\theta\theta}{}^p\}\mathrm{d}z + \int_{\frac{h_e}{2}}^{\frac{h_e}{2}+h_p} \frac{[\cos\left(\frac{\pi}{h_p}\rho\right)]^2}{(R+z)}\{\epsilon_{\theta\theta}{}^p, m_{\theta\theta}{}^p, \mu_{\theta\theta}{}^p\}\mathrm{d}z$$

$$\{A_{32}, A_{33}, A_{34}, A_{35}, A_{36}, A_{37}\} = \int_{-\frac{h_e}{2}}^{+\frac{h_e}{2}} \frac{E}{2(1+\upsilon)}l'^2\frac{1}{2(R+z)}\{1, \frac{1}{R+z}, \frac{z}{R+z}, \frac{1}{(R+z)^2}, \frac{(R - z^2}{(R+z)^2}\}dz + \int_{-\frac{h_e}{2}-h_p}^{-\frac{h_e}{2}} \frac{E}{2(1+\upsilon)}l'^2\frac{1}{2(R+z)}\{1, \frac{1}{R+z}, \frac{z}{R+z}, \frac{1}{(R+z)^2} \frac{z^2}{(R+z)^2}\}dz + \int_{\frac{h_e}{2}}^{\frac{h_e}{2}+h_p} \frac{E}{2(1+\upsilon)}l'^2\frac{1}{2(R+z)}\{1, \frac{1}{R+z}, \frac{z}{R+z}, \frac{1}{(R+z)^2}, \frac{z^2}{(R+z)^2}\}dz$$